# COMPLEX HYDRIDES – A New Frontier for Future Energy Applications

## Poster ID BES012

Vitalij K. Pecharsky,[1] Marek Pruski,[2] L. Scott Chumbley,[3]

Duane D. Johnson,[4] Takeshi Kobayashi[5]

[1] FWP Leader: Ames Laboratory, 253 Spedding Hall, Ames, IA 50011, e-mail: vitkp@ameslab.gov, Tel.: 515-2948220; [2] PI: Ames Laboratory, 230 Spedding Hall, Ames, IA 50011, e-mail: mpruski@iastate.edu, Tel.: 515-2942017; [3]PI: Ames Laboratory, 214 Wilhelm Hall, Ames, IA 50011, e-mail: chumbley@iastate.edu, Tel.: 515-2947903; [4] PI: Ames Laboratory, 311 TASF, Ames, IA 50011, e-mail: ddj@ameslab.gov, Tel.: 515-2949649; [5] Ames Laboratory, 229 Spedding Hall, Ames, IA 50011, e-mail takeshi@iastate.edu, Tel. 515-2946823.

DOE Program Officer: Dr. Refik Kortan,  e-mal: Refik.Kortan@Science.DOE.gov, Tel.: 301-9033308

# COMPLEX HYDRIDES – A New Frontier for Future Energy Applications

V.K. Pecharsky (FWP leader), M. Pruski (PI), L.S. Chumbley (PI), D.D. Johnson (PI) and T. Kobayashi

## Objectives:

- Examine and compare mechanical energy- and thermal energy-driven phase transformations in model complex hydrides at and away from thermodynamic equilibrium to enable their future use.

- Establish the nature and structure of the products and intermediates using high resolution solid-state NMR, electron microscopy, as well as first principles theory and modeling.

- Provide a fundamental understanding of the nature of hydrogen bonding and formation, structure, and stability of the model systems, the effects of mechanical energy, temperature, and pressure in controlling the nature of hydrogen-metal bonds.

- Identify events critical to achieving reversibility of hydrogen in model systems under mild conditions.

## Outline:

# Mechanochemistry: a powerful tool for non-equilibrium processing of metal hydrides

## Mechanochemistry: reactive ball milling

- Combines pressure and shear in a complex, stochastic process
- Potentially leads to local temperature and pressure changes (both may be very large)
- Mechanical energy is converted into strain energy, which is relieved via
  - Deformation of chemical bonds
  - Vibrational excitations of atoms
  - Electronic excitations and ionization
  - Dissociation and rearrangement of chemical bonds
  - Mass transfer is very rapid, "ballistic diffusion"
  - Continuous creation of defects and vacancies

## Other advantages

- Easy scale-up from research (milligram) to production level (kilogram)
- Direct hydrogenation possible, pristine products, eliminates expensive purification steps
- Easy access of different pressure, time and energy regimes and milling modes

**Our Approach:**



Reactive ball milling of $MgB_2$ (in Fritsch P7 miller) at temperatures between -30°C–RT and 1–350 bar pressure.
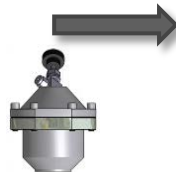
Structural characterization and phase analysis by XRD, TG-DSC, TEM and SSNMR (H, $^{11}B$, $^{27}Al$, etc.)

Capacity, thermodynamics, kinetics and cycle life measurements.

# Characterization of metal hydrides by solid-state NMR spectroscopy

The solid-state NMR studies use state-of-the-art high-resolution methods, **some of which were developed in our group at Ames Laboratory.** We specialize in the studies of both spin-1/2 and half-integer quadrupolar nuclei:

- **spin-1/2 nuclei:** new experiments utilizing ultrafast MAS; improved pulse sequences for 2D heteronuclear correlation (HETCOR) methods

- **half-integer quadrupolar nuclei:** multiple-quantum magic angle spinning (MQMAS); studies of interatomic correlations under high resolution

**These methods provide:**

- improved sensitivity and resolution

- direct chemical shift information and quadrupolar parameters

- improved basis for structural characterization in crystalline and amorphous phases

**Our group collaborates with Varian (now Agilent Technologies) on refining of the prototype probes. Part of this effort is sponsored by Ames Laboratory Royalty Funding. This research continues to drive the development of new NMR methodologies**

THE Ames Laboratory
*Creating Materials & Energy Solutions*
U.S. DEPARTMENT OF ENERGY

Agilent Technologies

# Characterization of metal hydrides by solid-state NMR spectroscopy

**Solid-state NMR studies of metal hydrides are used in concert with other characterization methods (XRD, PCT-RGA) and theoretical modeling to obtain structural and dynamic information about crystalline and amorphous phases in these complex materials and mechanisms of dehydrogenation and rehydrogenation**

**Our approach:**

- **measure 1D and 2D NMR spectra of $^1H$, $^7Li$, $^{11}B$, $^{23}Na$, $^{27}Al$ and other nuclei in hydrides processed under various conditions and in reference compounds**

- **obtain chemical shifts and quadrupolar parameters (for spins > 1/2) to identify the coordination geometries and chemical structures**

- **carry out the additional SSNMR experiments to probe interatomic correlations, molecular motions, etc.**

- **utilize the results of XRD studies of crystalline structures**

- **refine the structures using molecular modeling and DFT calculations**
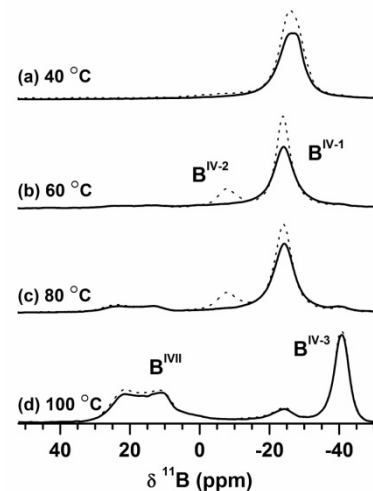


$^{11}B$ MAS

$^{11}B$ MQMAS

DFT ($\delta_{CS}$, $P_Q$)

4
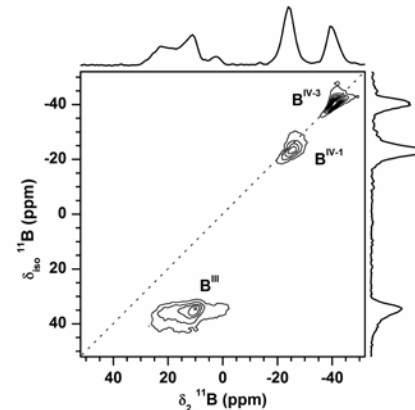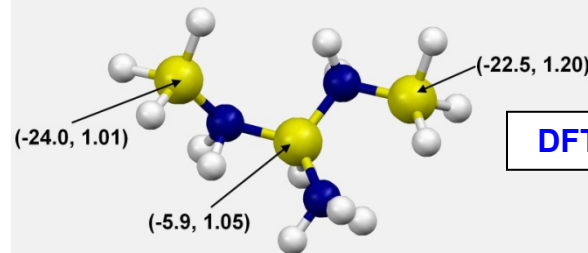
# Thermal dehydrogenation of $LiAlH_4$ - $LiNH_2$

- Light weight complex hydrides, such as alanates $[AlH_4]^-$, amides $[NH_2]^-$, imides $[NH]^{2-}$ and borohydrides $[BH_4]^-$ are very desirable for hydrogen storage, because of high hydrogen content, e.g., 10.5 wt% for $LiAlH_4$, 8.7 wt% for $LiNH_2$ and 18.1 wt% for $LiBH_4$

- In our earlier work [1], the high-energy ball milling of the mixture $MAlH_4$ - $MNH_2$ ($M$ = Li or Na) yielded 5.2 wt% of H for $LiNH_2$ and 4.3 wt% of H for $NaNH_2$

- Here, the thermochemical dehydrogenation of $LiAlH_4$ - $LiNH_2$ has been studied by XRD and SSNMR [2]

**TPD**

**XRD**

**$^7$Li NMR**

**$^{27}$Al NMR**
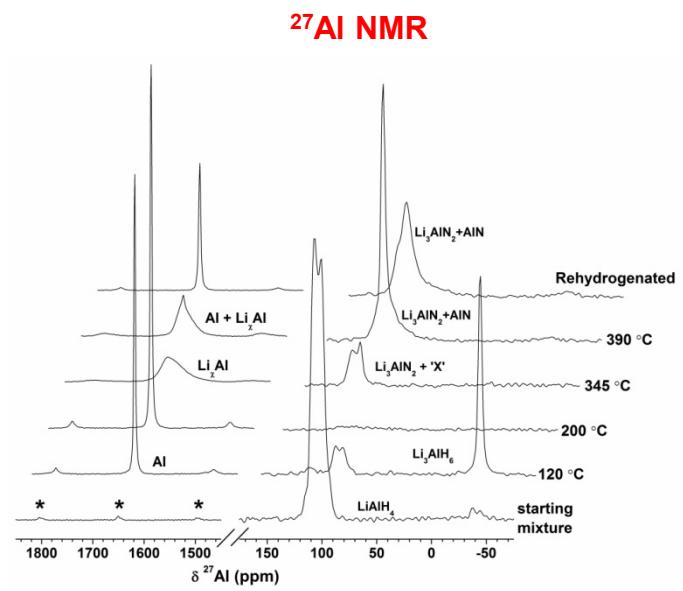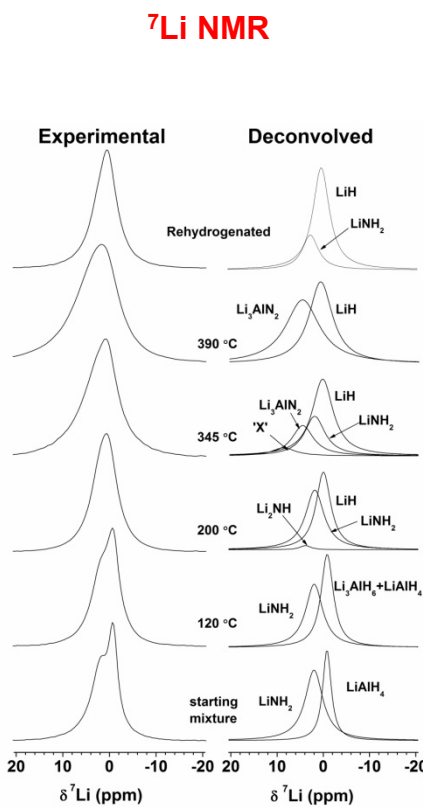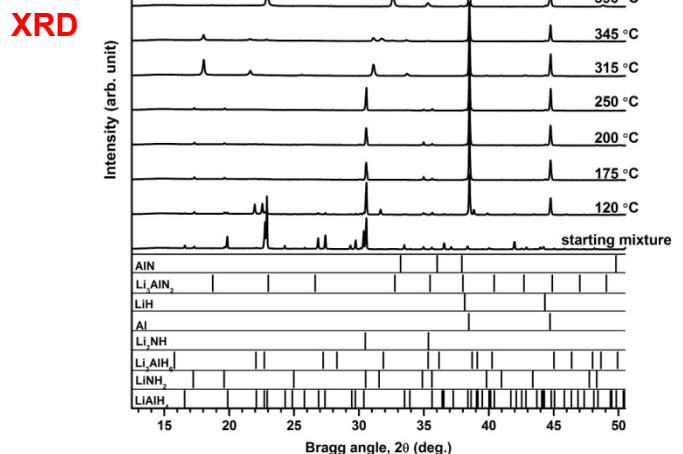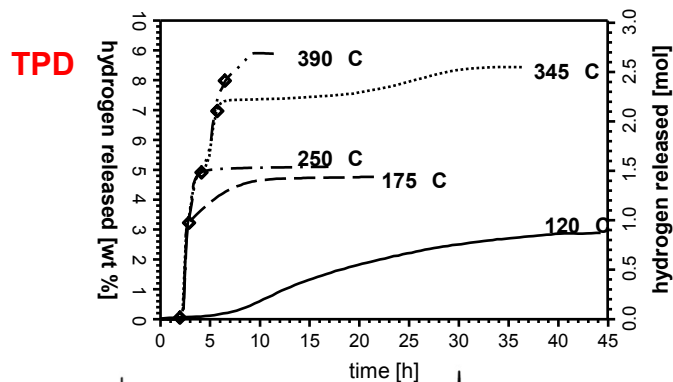
[1] Dolotko, O.; Zhang, H.Q.; Ugurlu, O.; Wiench, J.W.; Pruski, M.;Chumbley, L.S.; Pecharsky, V.K. *Acta Materialia*, **2007**, *55*, 3121-3130.
[2] Dolotko, O.; Kobayashi, T.; Wiench, J.W.; Pruski, M.;Chumbley, L.S.; Pecharsky, V.K. *Int J Hydrogen Energy*, **2011**, *36*, 10626-10634

# Thermal dehydrogenation of $LiAlH_4$ - $LiNH_2$: product analysis by 2D NMR experiments

- The resonance frequencies in MAS NMR spectra of quadrupolar nuclei (I > 1/2) depend on the chemical shifts ($\delta_{CS}$) and quadrupole induced shifts ($\delta_{QIS}$). The MQMAS technique yields the precise values of $\delta_{CS}$ and $\delta_{QIS}$

- The $^{27}Al$ 3QMAS and 2D HETCOR experiments detected the formation of $Li_3AlN_2$ and intermediate "X" at 345 C.

- At 390 C, AlN formed as a final product, while the intermediate disappeared.
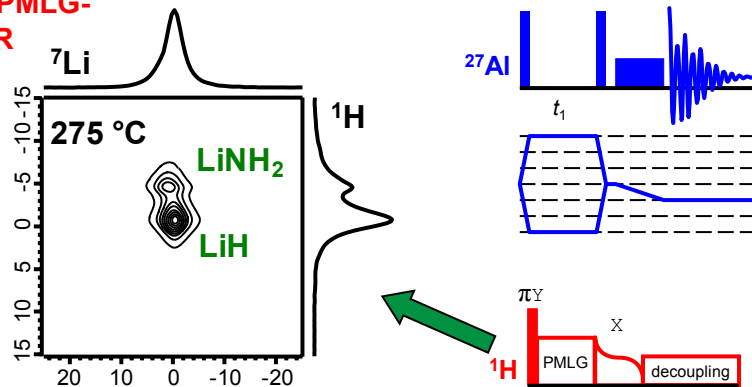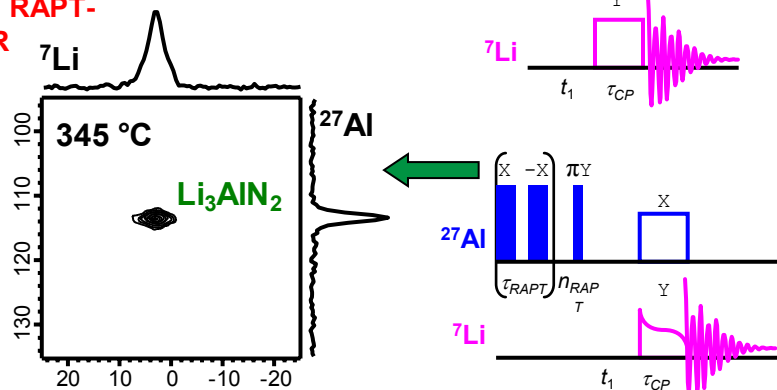
Reference samples

Heated samples

$^1H \rightarrow {}^7Li$ PMLG-HETCOR

$^7Li$

$^1H$

275 °C   $LiNH_2$   LiH

$^{27}Al \rightarrow {}^7Li$ RAPT-HETCOR

$^7Li$

$^{27}Al$

345 °C   $Li_3AlN_2$

$^{27}Al$

$t_1$

$\pi_Y$   X

$^1H$   PMLG   decoupling

Y

$^7Li$   $t_1$   $\tau_{CP}$

X  −X   $\pi_Y$

$^{27}Al$   $\tau_{RAPT}$   $n_{RAPT}$   X

$^7Li$   Y   $t_1$   $\tau_{CP}$

$LiAlH_4$

345°C   $Li_3AlN_2$   "X"

$Li_3AlN_2$

390°C   $Li_3AlN_2$

AlN

390° rehydrogenated   AlN   "X"

6
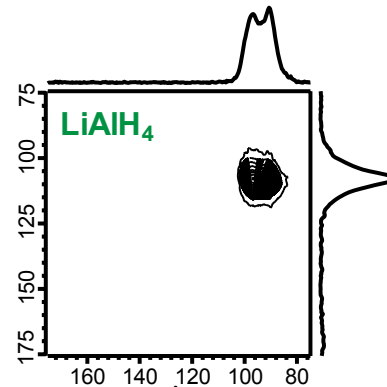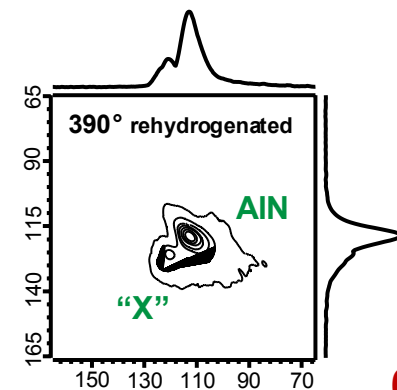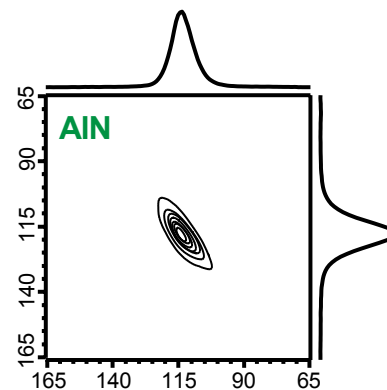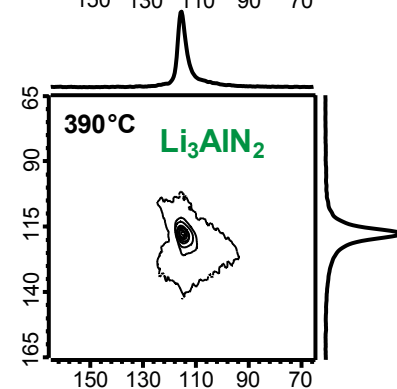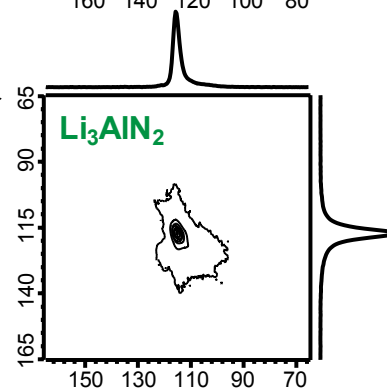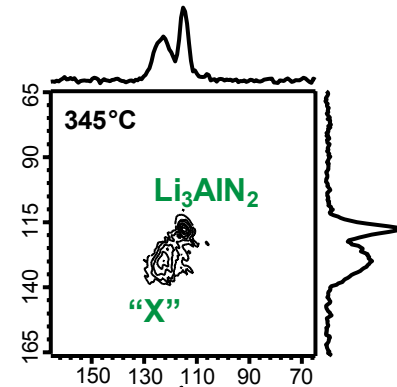
# Thermal dehydrogenation of $LiAlH_4$ - $LiNH_2$: reaction mechanism

(a) $^{27}Al \rightarrow {}^7Li$ RAPT-HETCOR, (b) $^{27}Al$ MAS NMR and (c) $^7Li$ MAS NMR show the formation of intermetallic compound, $\alpha$-LiAlx, as an intermediate.



(a) $^7Li$ / $^{27}Al$ — 345 °C

(b) Al / $\alpha$-LiAl$_x$ / Al — Physical mixture, 175 °C, 315 °C, 345 °C, 390°C rehydrogenated

(c) $\alpha$-LiAl$_x$

**Reactions:**

120 °C: $LiAlH_4 \rightarrow 1/3 Li_3AlH_6 + 2/3 Al + H_2$

150-250 °C: $Li_3AlH_6 \rightarrow 3LiH + Al + 3/2 H_2$

< 250 °C: $LiAlH_4 \rightarrow 3LiH + Al + 3/2 H_2$

315-345 °C: $2LiNH_2 + LiH + Al \rightarrow Li_3AlN_2 + 5/2 H_2$

$xLiH + Al \rightarrow Li_xAl + x/2 H_2$

390 °C: $3LiNH_2 + 2Al \rightarrow Li_3AlN_2 + AlN + 3H_2$

**Overall:** $LiAlH_4 + LiNH_2 \rightarrow 1/2 Li_3AlN_2 + 1/2 Al + 1/2 LiH + 11/4 H_2$
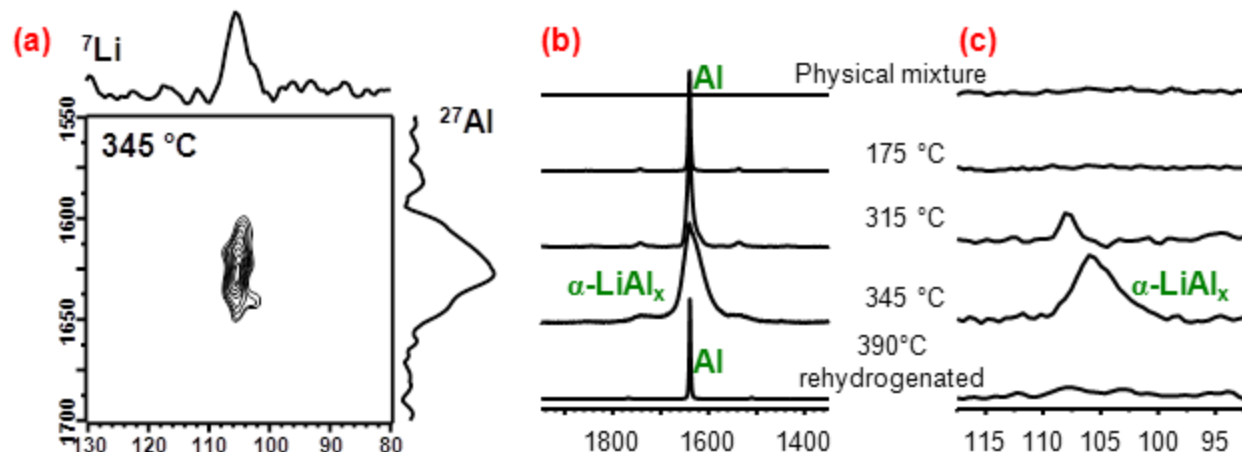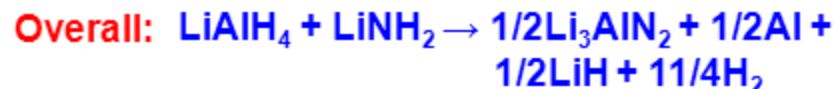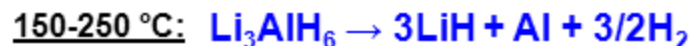
**Conclusions:**

- Below 250 °C, the alanate decomposes into Al, LiH and $H_2$, through the formation of $Li_3AlH_6$, whereas the amide remains intact. The release of gaseous hydrogen corresponds to ~5 wt%.

- Above 250 °C, additional ~4 wt% of hydrogen is produced in a solid-state reaction among $LiNH_2$, LiH and metallic Al, through the formation of intermetallic Li-Al binary alloy and an unidentified intermediate.

- The overall reaction of the thermochemical transformation of the $LiAlH_4$ - $LiNH_2$ mixture results in the production of $Li_3AlN_2$, metallic Al, LiH, and the release of 9 wt% of hydrogen.

Dolotko, O.; Kobayashi, T.; Wiench, J.W.; Pruski, M.; Chumbley, L.S.; Pecharsky, V.K. *Int J Hydrogen Energy*, **2011**, *36*, 10626-10634

# Li-assisted thermal dehydrogenation of $Li_3AlH_6$-$3NH_3BH_3$

## Dehydrogenation of ammoniaborane (AB)

- Hydrogen content of AB (19.6 wt%) exceeds by a factor of more than two the 9.0 wt% target set by DOE for 2015. AB is stable at ambient temperature, however 2/3 of available $H_2$ is released upon thermolysis below 200 °C.

- Practical application of AB as $H_2$ source suffers from sluggish dehydrogenation kinetics at moderate temperatures (184 kJ/mol) [1], concurrent emission of borazine and diborane, and the absence of effective methods for regeneration of spent AB.

- In the earlier study of dehydrogenation from the LiH - AB mixture, the activation energy was lowered to 75 kJ/mol [2]. However, the detailed reaction mechanism has not been identified. Inspired by this report, the dehydrogenation of the $Li_3AlH_6$ - 3AB mixture was examined and the detailed reaction mechanism was studied by the extensive use of SSNMR spectroscopy and theoretical calculations.
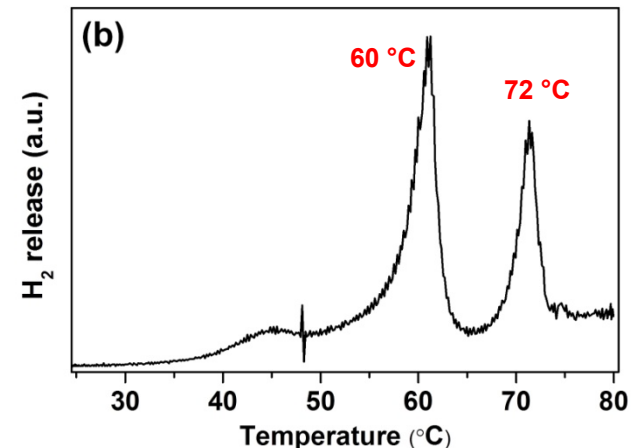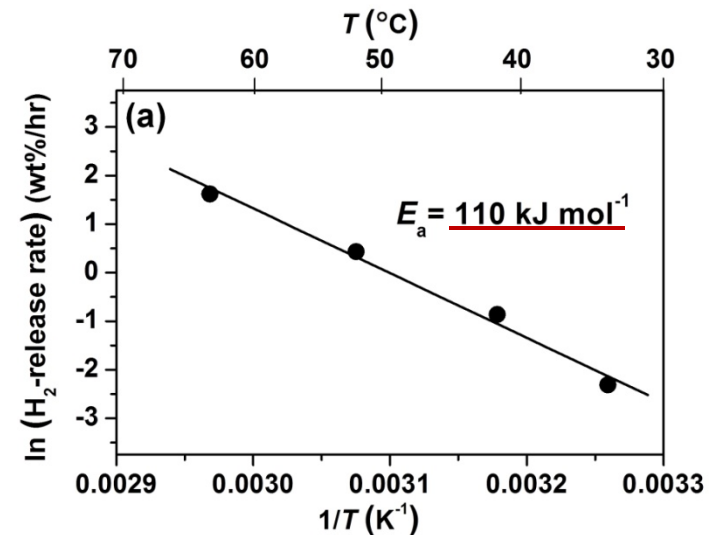
$E_a$ = 110 kJ mol$^{-1}$

[1] Gutowska, A; Li, L.Y.; Shin, Y.S.; Wnag, C.M.M.; Li, X.H.S.; Linehan, J.C.; Smith, R.S.; Kay, B.D.; Schmid, B.; Shaw, W.; Gutowski, M.; Autrey, T. *Angew. Chem. Int. Ed.* **2005**, *44*, 3578-3582; [2] Kang, X. D.; Fang, Z. Z.; Kong, L. Y.; Cheng, H. M.; Yao, X. D.; Lu, G. Q.; Wang, P. *Adv. Mater.* **2008**, *20*, 2756-2759.

- The reaction products were analyzed using SSNMR measurements.

- The solid-state reaction between $Li_3AlH_6$ and $NH_3BH_3$ starts at 40 °C.

- ~75 % of $Li_3AlH_6$ remains intact after treatment below 100 °C.

- The ~10 ppm $^{27}Al$ signal is assigned to $AlH_3$. This signal almost disappeared at 80 °C, whereas the signal assigned to metallic Al emerged.

- The tetrahedral site $B^{IV-2}$ assigned to branched poly-amonoborane (see below) was observed at 60 °C; however, polyaminoborane species were detected in the pristine AB sample.

$Li_3AlH_6$ - $3NH_3BH_3$ and reference compounds

$^{27}Al$ NMR

$^{11}B$ NMR

Kobayashi, T.; Hlova, I.Z.; Singh, N.K.; Pecharsky, V.K.; Pruski, M. *Inorg. Chem.*, **2012**, *51*, 4108-4115.

9
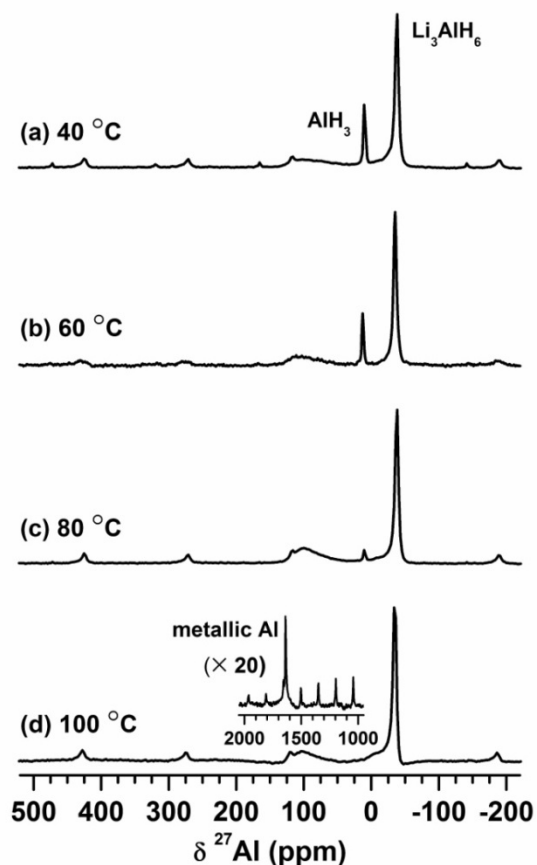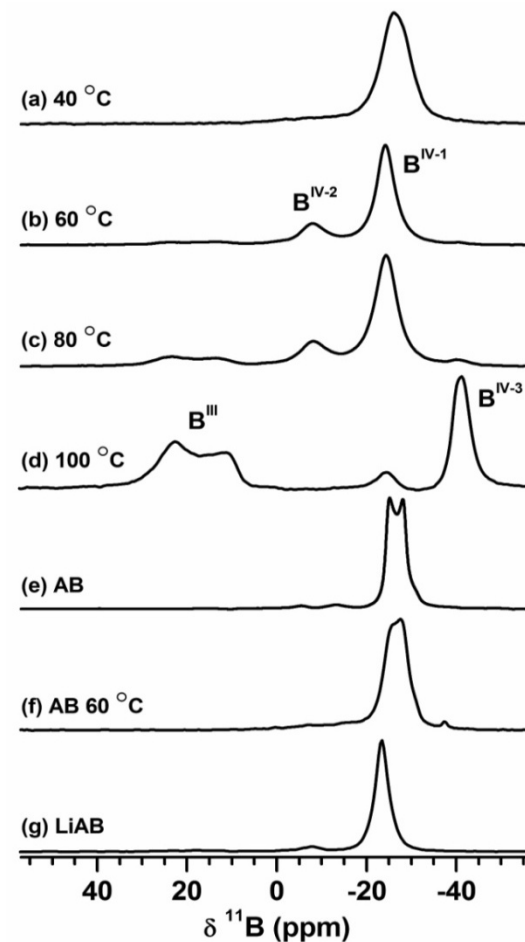
# Li-assisted thermal dehydrogenation of $Li_3AlH_6$-$3NH_3BH_3$: 2D $^{11}B$ 3QMAS NMR and theoretical calculations

Based on $^{11}B$ 3QMAS NMR and theoretical calculations, $B^{IV-1}$ and $B^{IV-2}$ were assigned to $B$H(−N≡)$_3$ and $(LiNH_3BH_3)_x(NH_3BH_3)_{1-x}$, respectively.

## $^{11}B$ 3QMAS



## Theoretical calculations
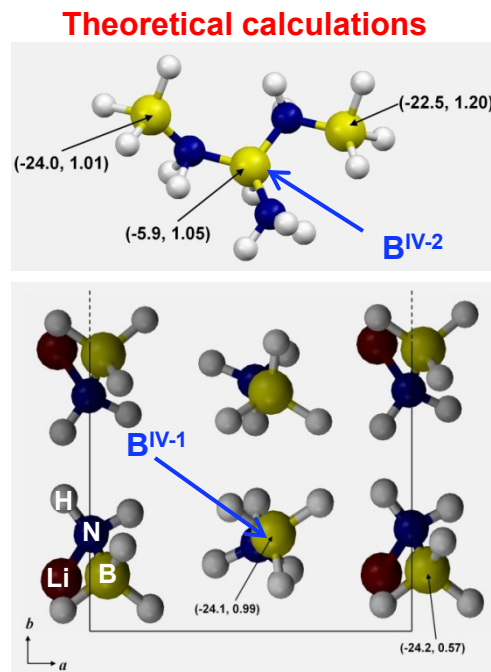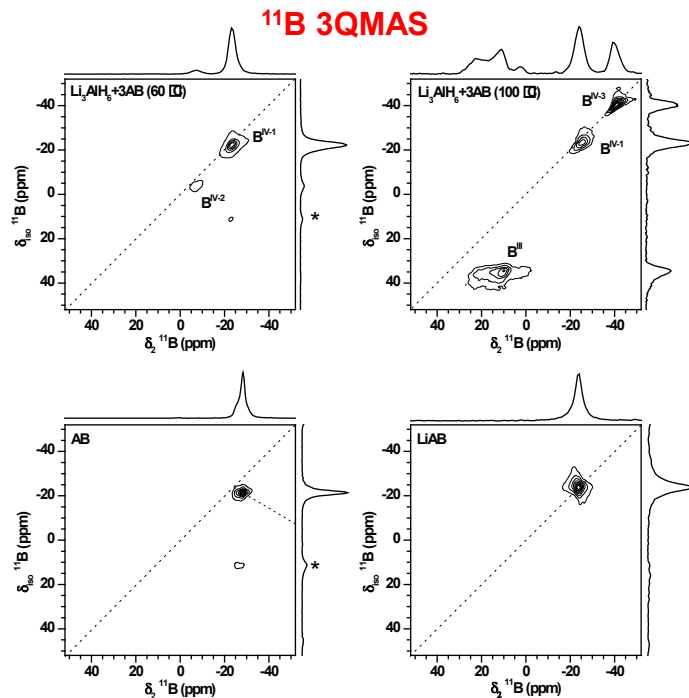


| sample | site | $\delta_{CS}$ | $\delta_{QIS}$ | $P_Q$ (MHz) |
|--------|------|---------------|----------------|-------------|
| 60 °C | $B^{IV-1}$ | -23.3 | 1.4 | 1.0 |
| | $B^{IV-2}$ | -5.9 | 2.6 | 1.3 |
| 100 °C | $B^{IV-1}$ | -24.0 | 1.2 | 0.9 |
| | $B^{IV-3}$ | -40.7 | 0.2 | 0.4 |
| AB | | -23.9 | 3.7 | 1.6 |
| LiAB | | -24.1 | 0.46 | 0.5 |

| sample | site | $\delta_{CS}$ | $P_Q$ (MHz) |
|--------|------|---------------|-------------|
| $c$-LiAB | $LiNH_2BH_3$ | -22.7 | 0.59 |
| $c$-AB | $NH_3BH_3$ | -23.8 | 1.51 |
| $c$-LiAB·AB | $LiNH_2BH_3$·AB | -24.1 | 0.57 |
| | LiAB·$NH_3BH_3$ | -24.2 | 0.99 |
| LiAB | $LiNH_2BH_3$ | -22.4 | 0.59 |
| AB | $NH_3BH_3$ | -21.3 | 1.45 |

10

# Li-assisted thermal dehydrogenation of $Li_3AlH_6$-$3NH_3BH_3$: reaction mechanisms

- ^{11}B 3QMAS NMR and theoretical calculations suggested the formation of intermediate compound between AB and LiAB, $(LiNH_2BH_3)_x(NH_3BH_3)$.

- This intermediate compound accelerates the formation of polyaminoborane, which can be explained by the earlier theoretical study of LiAB [1]. The formation of polyaminoborane was observed in the mixture at as low as 60 C but was not observed in pristine AB.

- The formed polyaminoborane has branched structure, whereas linear polyaminoborane was not observed. This indicates that the dehydrogenation mechanism of the $Li_3AlH_6$ - 3AB mixture differs from that of pristine AB.

- The proposed reaction mechanism is as follows [2]:

**Formation of intermediate compound**

$$x/3Li_3AlH_6 + NH_3BH_3 \rightarrow (LiNH_2BH_3)x(NH_3BH_3)_{1-x} + x/3AlH_3 + xH_2$$

**Formation of polyaminoborane**

$$LiNH_2BH_3 + NH_3BH_3 \rightarrow NH_3BH_2–NH_2BH_3 + LiH$$

$$NH_3BH_2–NH_2BH_3 + LiNH_2BH_3 \rightarrow NH_3BH(NH_2BH_3)_2 + LiH$$
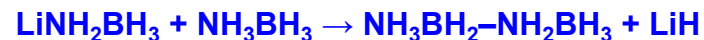
**Formation of trigonal boron ($B^{III}$ sites)**

$$NH_3BH(NH_2BH_3)_2 \rightarrow NH_3B(=NHBH_3)(NH_2BH_3) + H_2$$

- The detailed reaction mechanism, in particular the role of lithium revealed in this study, opens up opportunities for exploring new classes of hydrogen storage materials (both pure compounds and mixtures) and strategies of their utilization.

[1] Wu, H.;Zhou, W.; Yildirim, T. *J. Am. Chem. Soc.* **2008**, *130*, 14834-14839.
[2] Kobayashi, T.; Hlova, I.Z.; Singh, N.K.; Pecharsky, V.K.; Pruski, M. *Inorg. Chem.,* **2012**, *51*, 4108-4115.

# Mechanochemical hydrogenation of MgB$_2$: effect of ball-milling time

- MgB$_2$ + 4H$_2$ → Mg(BH$_4$)$_2$; hydrogen content of Mg(BH$_4$)$_2$ - 14.8 wt%.
- In the earlier study, ~75% of MgB$_2$ was thermally hydrogenated to Mg(BH$_4$)$_2$, but the process required very severe conditions (950 bar of H$_2$ at 400 °C, 108 h) [1].
- Mechanochemical synthesis at lower pressure is possible. [2]
- In the present study, ~80 % of MgB$_2$ was mechanochemically hydrogenated to form Mg(BH$_4$)$_2$ with 350 bar H$_2$ for 60 h at room temperature. Over 70 % of total conversion took place in the first 7-15 h of ball-milling.

| Time (h) | species (%) | | | H$_2$ desorption below 390 °C (wt%) |
|---|---|---|---|---|
| | MgB$_2$ | [B$_{12}$H$_{12}$]$^{2-}$ | BH$_4^-$ | |
| 3.5 | 78.7 | 8.7 | 12.6 | 1.3 |
| 7 | 33.6 | 13.2 | 53.2 | 1.9 |
| 15 | 30.1 | 8.0 | 61.9 | 3.0 |
| 30 | 27.3 | 1.5 | 71.1 | 3.6 |
| 45 | 25.0 | 1.1 | 73.9 | 3.9 |
| 60 | 17.7 | 1.6 | 80.7 | 3.9 |



$^{11}$B NMR spectra of MgB$_2$ ball-milled under 350 bar H$_2$ at room temperature
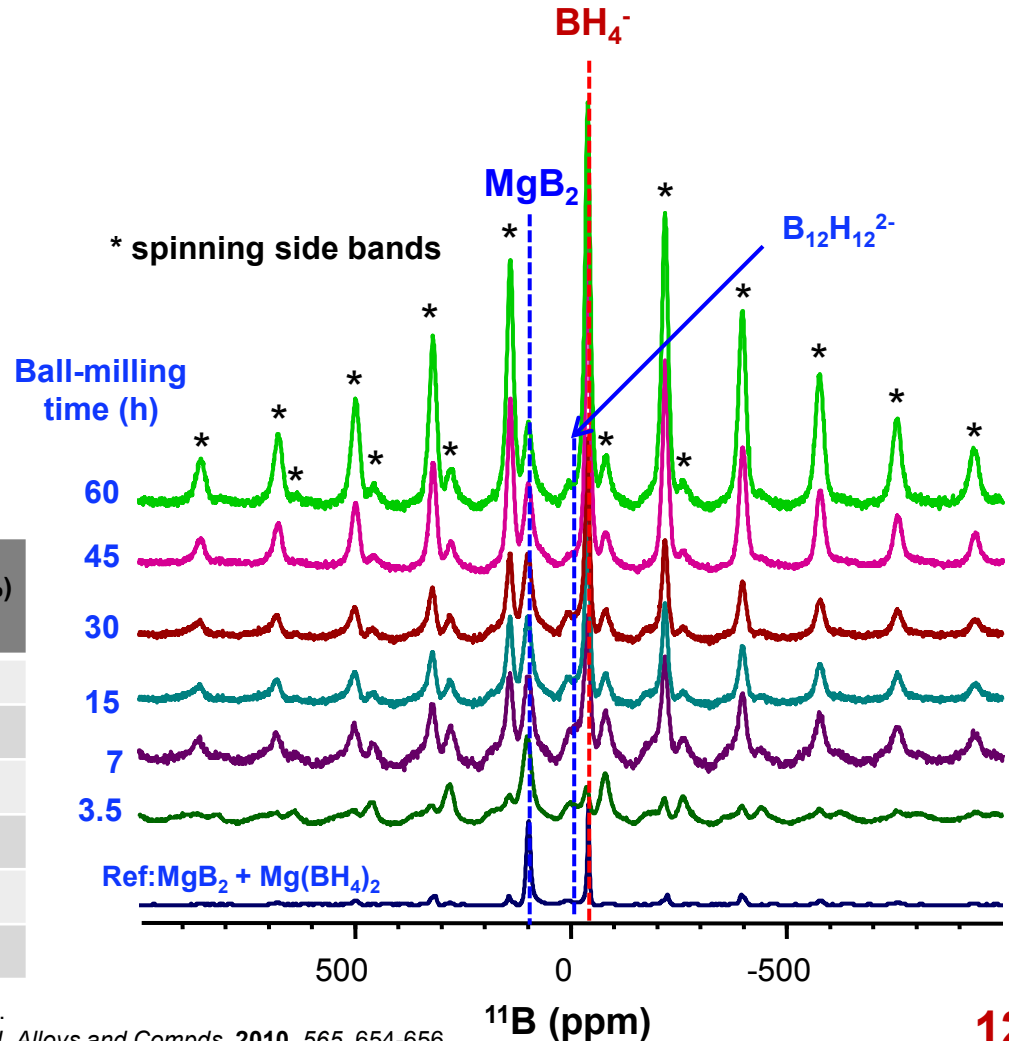
[1] Severa, G.; Rönnebro E.; Jansen M., *Chem. Commun.* **2010**, *46*, 421-423.
[2] Li H.-W.; Matunaga, T.; Yan, Y. Makawa, H.; Ishikiriyama, M.; Orimo, S, *J. Alloys and Compds,* **2010**, *565*, 654-656.

# Mechanochemical hydrogenation of MgB$_2$: effect of H$_2$ pressure

- **Mechanochemical hydrogenation of MgB$_2$ allows significant reduction of H$_2$ pressure. The reaction proceeded at as low as 50 bar of H$_2$.**

- **Transformation of Mg(B$_{12}$H$_{12}$) to Mg(BH$_4$)$_2$ requires longer ball-milling time, rather than high H$_2$ pressure.**

| H$_2$ (bar) | species (%) | | | H$_2$ desorption below 390 °C (wt%) |
|---|---|---|---|---|
| | MgB$_2$ | [B$_{12}$H$_{12}$]$^{2-}$ | BH$_4^-$ | |
| 50 | 48.7 | 7.4 | 43.9 | 1.7 |
| 100 | 46.3 | 4.0 | 49.7 | 2.1 |
| 150 | 39.1 | 9.8 | 51.2 | 2.6 |
| 200 | 37.3 | 8.2 | 54.5 | 2.8 |
| 250 | 36.8 | 5.4 | 57.9 | 3.1 |
| 300 | 35.8 | 5.0 | 59.2 | 3.2 |
| 350 | 27.3 | 8.0 | 61.9 | 3.0 |



$^{11}$B NMR spectra of MgB$_2$ ball-milled (15 h) under various H$_2$ pressure at room temperature

13
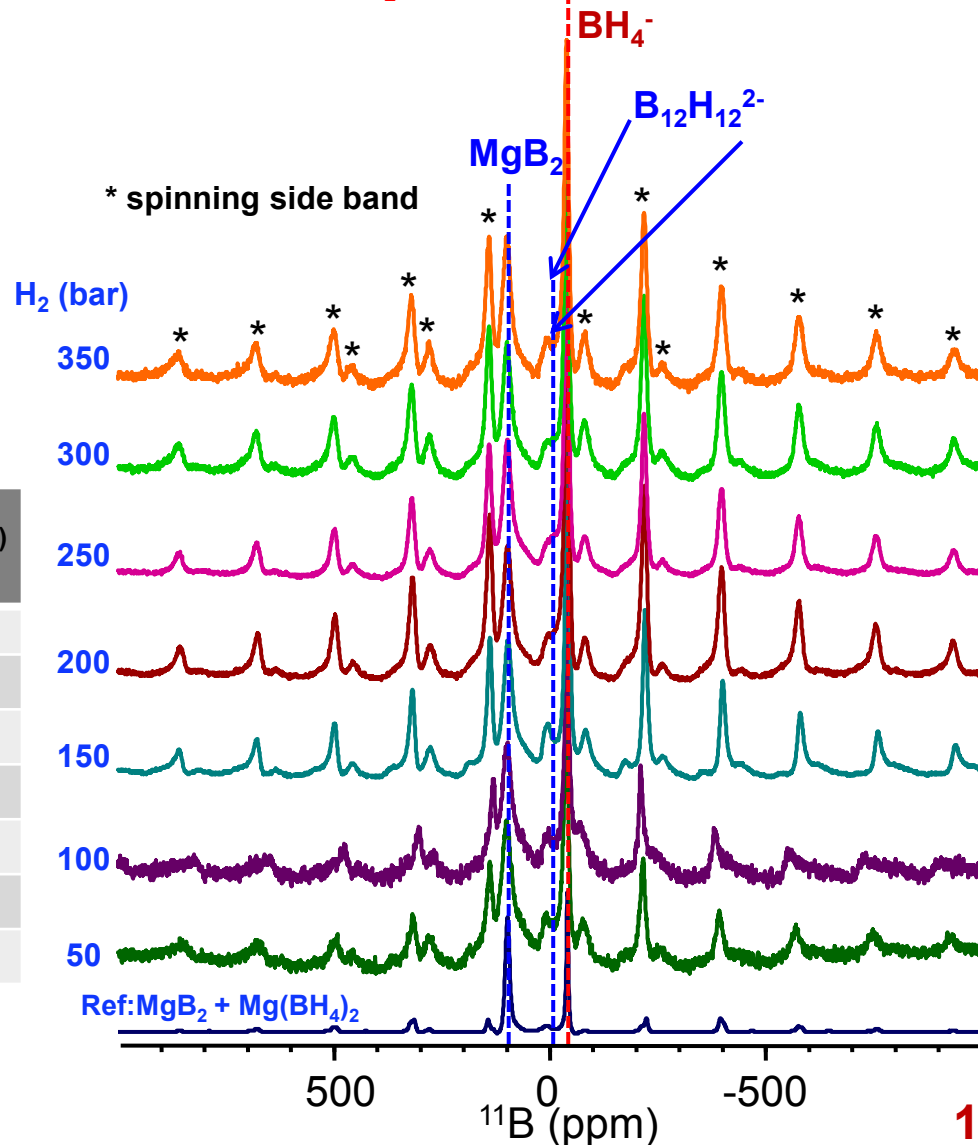
# Mechanochemical hydrogenation of $MgB_2$: dehydrogenation and rehydrogenation

- The produced $Mg(BH_4)_2$ was thermally **dehydrogenated** to form $MgB_2$ and $Mg(B_{12}H_{12})$ with desorption of ~4 wt% $H_2$ below 400 C. Dehydrogenation was not completed due to the formation of stable compound, $Mg(B_{12}H_{12})$.

- Up to 70–80 % of initial capacity was retained upon 2nd and 3rd recharging by reactive milling.

**Thermal dehydrogenation from the ball-milled products**
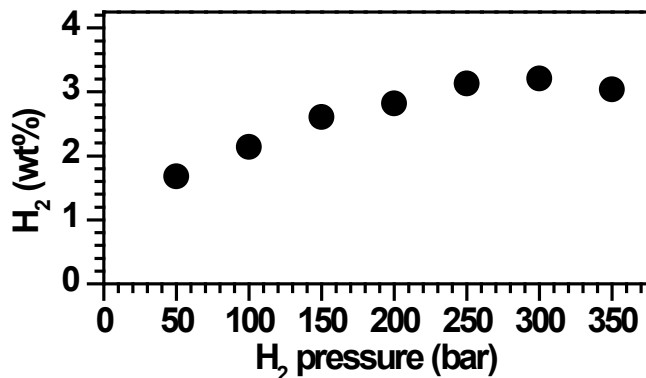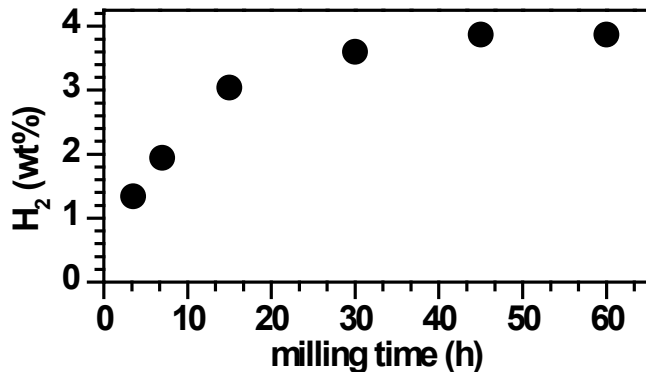
**$^{11}$B NMR spectra of hydrogenated $MgB_2$, followed by dehydrogenation and rehydrogenation**
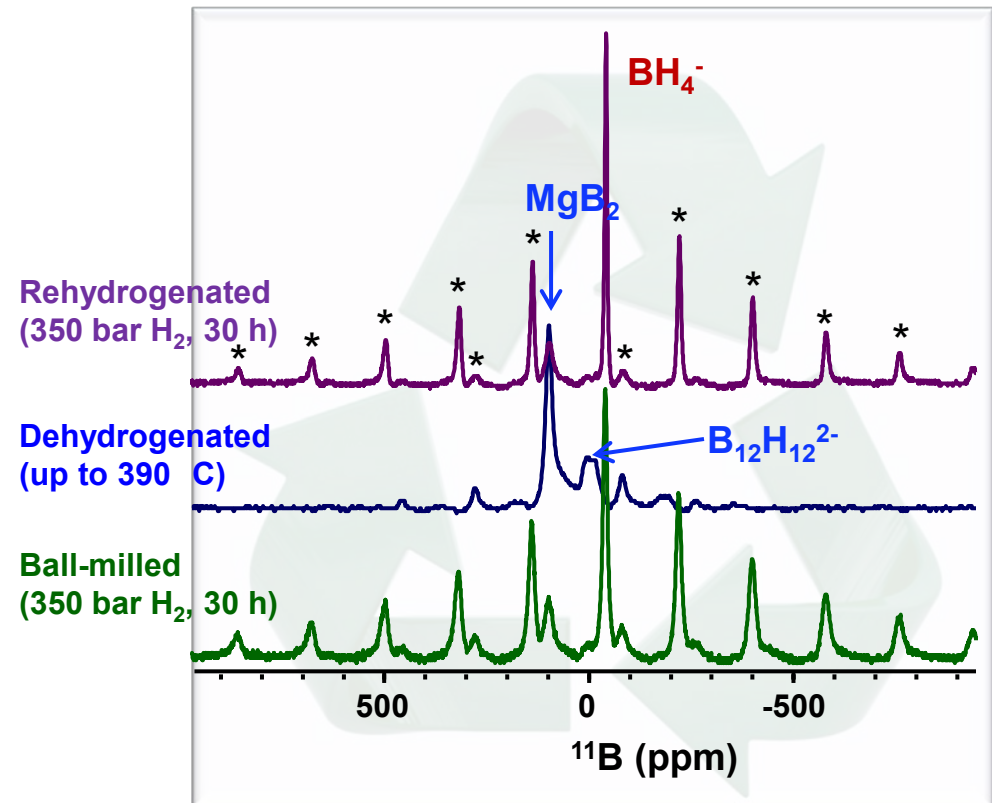
# Ti-doped MgH$_2$(110) H-desorption path



**Initial State**

*Top view*

*Side view*

Bulk-diffusion assist
Low barrier

Transition state
push/pull
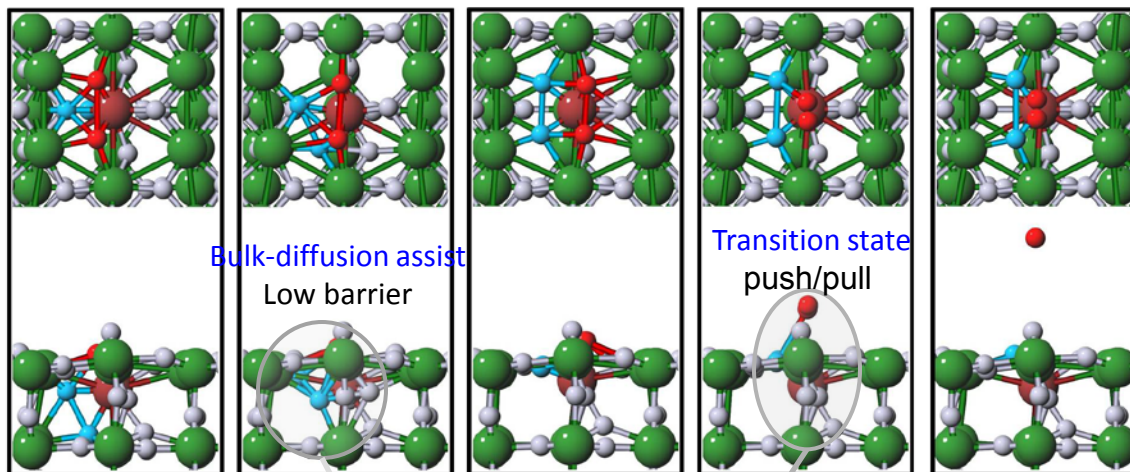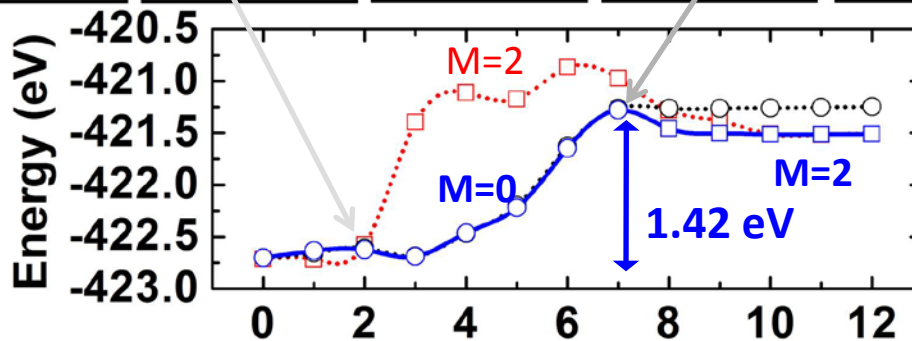
**Final State**

Potential Energy Surface Images along pathway

- **Ti-doping yields 0.41 eV (22%) drop in barrier** – **agrees with observed 0.46 eV.***

- Ti-assisted desorption of H$_2$ has a spin transition from M = 0 to 2 $\mu_B$, with early diffusion of 2$^{nd}$ layer H preferring M = 0 $\mu_B$.

- Final state prefers M = 2 $\mu_B$, with a change in HCN from 8→6.

*Wang and Johnson, J. Chem. Phys. C, 2012, online. **15**

**MgH$_2$(110) surface slab models**
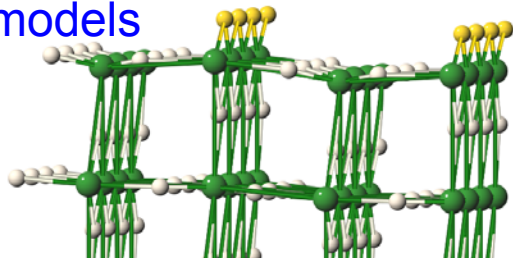


MgH$_2$(110) terrace w/ double H-M bonds
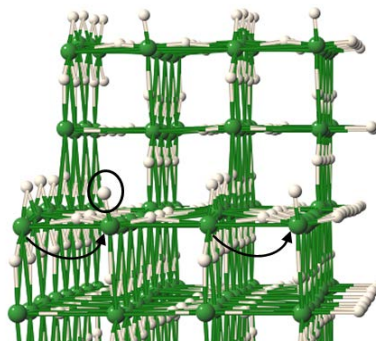


MgH$_2$(110) step w/ singly H-M bond
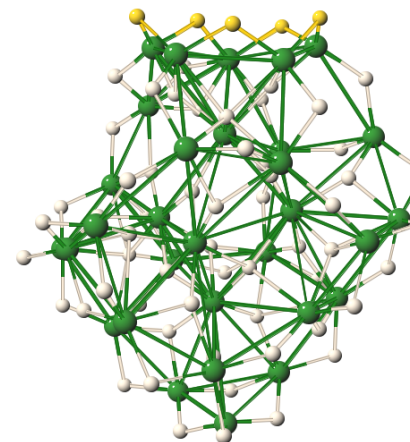


Mg$_{31}$H$_{62}$ NP from DFT simulated annealing

**From DFT energies, we find** NO SIZE EFFECTS on H-desorption enthalpies:

- H-Desorption energies are similar from nanoparticles (NPs) and bulk, i.e.,
  - ✓ NP vs bulk – single H-M bond: 148 kJ(mol-H$_2$)$^{-1}$ vs 140 kJ(mol-H$_2$)$^{-1}$
  - ✓ NP vs bulk – double H-M bond: 252 kJ(mol-H$_2$)$^{-1}$ vs 231 kJ(mol-H$_2$)$^{-1}$
  - ✓ **Ti-doped, double H-M bond:** 188 kJ(mol-H$_2$)$^{-1}$ vs 140 kJ(mol-H$_2$)$^{-1}$
- Surface step edges have the more favorable desorption site for MgH$_2$(110).
- Full H removal enthalpy for bulk: 58 kJ(mol-H$_2$)$^{-1}$, observed is 68 kJ(mol-H$_2$)$^{-1}$.
- Amorphous NP has the same **<u>bonding motifs</u>** as bulk surface, so no size effects.

**Structural motifs:**

2-D projection of bulk MgH$_2$(110) and NP


BULK


NP
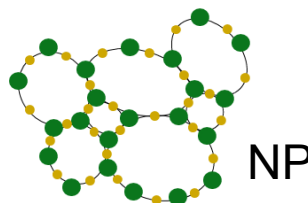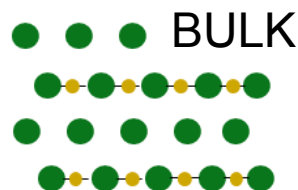
**Calculations performed using VASP-PW91**
- BULK: 400 eV cutoff and 8x8x12 k-points
- SLAB: 9 layers and 15 Å vacuum in 2x4 surf. cell
- Converged: 2 meV/atom (0.02 eV/Å) energy (forces)

*Reich, Wang, Johnson, 2012, submitted.

**16**

# Activations barriers in $Mg_{31}H_{62}$ NPs



**Nudged Elastic Band: 2H removal**

NP H-desorption Barrier
NP: 1.85 eV
Bulk: 1.84 eV

$Mg_{31}H_{62}$ Pair Correlatoin Binning

After $H_2$ release

Before $H_2$ release
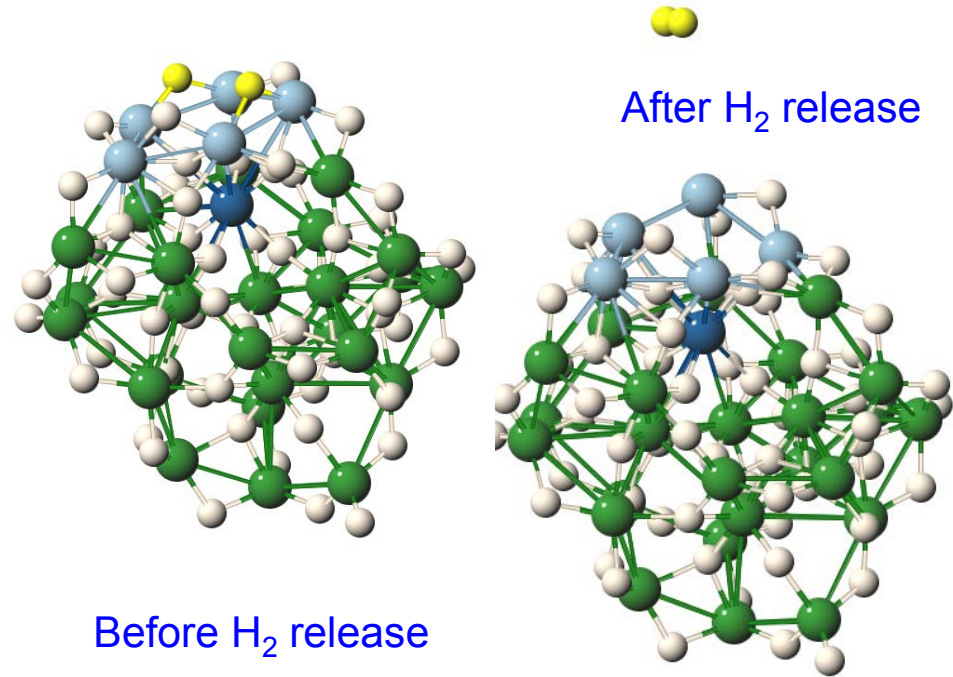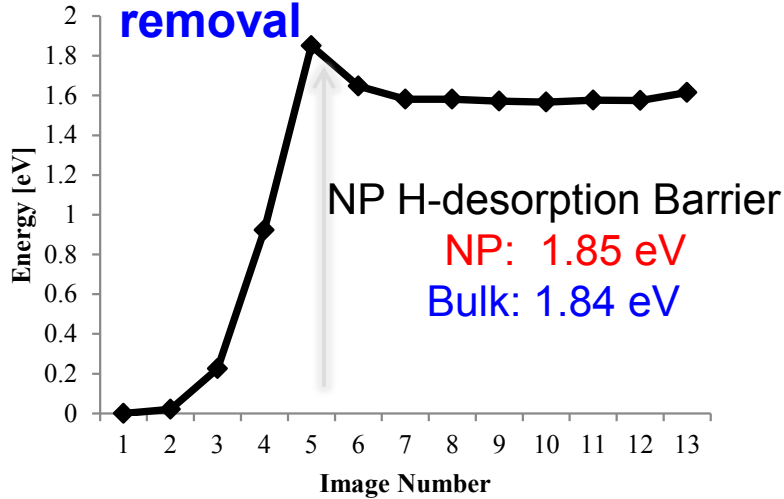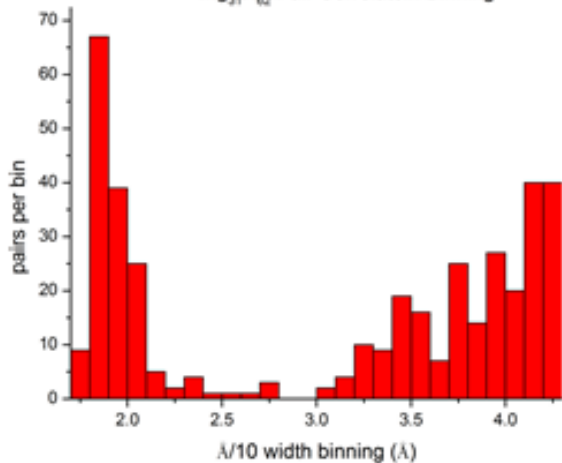
- NO SIZE EFFECT for H-desorption activation barriers.
- From pair bond distribution (left), many different sites and environments exist in NPs, plan to reveal trends for H removal.
- Dopants will have an effect, see previous slide.

*Reich, Wang, Johnson, 2012, in preparation.

17

# Future work and acknowledgements

**Future work:** more studies are needed to understand the structure – hydrogen storage activity relationships among promising complex hydrides. We will continue to rely upon integrating innovative transformations with state-of-the-art characterization and modeling, while pursuing new research directions, including:

- understanding of the direct mechanochemical synthesis of $AlH_3$ with high yields
- mechano- and thermo-chemical studies of $Mg(BH_4)_2$- and $Mg(NH_2BH_3)_2$-based systems
- development and testing of hybrid materials composed of complex hydrides and conventional intermetallic hydrogen absorbers
- use of mechanical energy to create non-equilibrium rehydrogenation pathways under low temperatures and hydrogen pressures
- development of improved characterization methods, such as in-situ solid-state NMR spectroscopy, and
- integration of experiments with theoretical modeling

**Special thanks to: V.P. Balema, F. Chen, K.W. Dennis, O. Dolotko, S. Gupta, I.Z. Hlova, P. Jena, N. Paulson, J.M. Reich, N.K. Singh, O. Ugurlu, L.L. Wang, J.W. Wiench and H. Zhang**

18